was obtained by preparing 7% polyacrylamide gel (without SDS) and run the gel in 0.01% SDS running buffer. In all experiments, the protein samples were prepared using loading dye without SDS, and bovine serum albumin (BSA, ~67 kD) and bovine gamma globulin (BGG, ~140 kD) were used as protein molecular weight markers.

Growth Study. Toxicity and cell viability profiles of *E. coli* cultures overexpressing the wild type *Hp* ND-AspRS, Chimera-D, and Chimera-N were evaluated according to the general procedure previously described. Briefly, a single colony was grown overnight in a 5 mL LB-ampicillin. This culture was used to inoculate 200 mL culture of the same medium to an OD_{600} of 0.05. The culture was incubated at 37 ^{0}C with agitation. The protein expression was induced by adding isopropyl-β-D-1-thiogalactopyranoside (IPTG) to a final concentration of 1 mM. Growth was monitored over the period of 7 hours. The reported data represents the average of experiments conducted in triplicate.

ผลการทดลอง

Swapping the N-terminal anticodon binding domain of Hp. ND-AspRS with those of E. coli AspRS and AsnRS does not drastically alter the secondary structure content of the enzyme. The AspRS and AsnRS belong to class IIb of all synthetases and exist as homodimeric proteins in nature. In order to investigate the contribution of the anticodon binding domain toward the tRNA specificity in *Hp* ND-AspRS, we decided to replace the N-terminal anticodon binding domain of the wild type *Hp* ND-AspRS with those of *E. coli* AspRS (Discriminating AspRS) and AsnRS, generating the Chimera-D and Chimera-N respectively. A closer look at the sequence similarity in the anticodon binding domain (104 amino acids long) revealed that the one from *E. coli* AspRS share a high percent similarity to those of *Hp* ND-AspRS (approximately 36%) where relatively lower similarity (approximately 14%) was observed between *E. coli* AsnRS and *Hp* ND-AspRS (Figure 1A and B). We hypothesized that the introduction of *E. coli* AspRS anticodon binding domain into *Hp.* ND-AspRS should yield a more stable and presumably more catalytically active enzyme due to the sequence similarity. In both cases of domain swapping, a unique restriction site must be introduced around the flexible loop that connects the anticodon binding domain and the catalytic domain (the hinge region). As it has been shown that this area of AspRS also interact with the tRNA substrate and, undeniably, contributes to its tRNA specificity, the restriction site must be introduced at the position where the amino acid is less conserved in order to avoid the interruption of substrate binding. In response to the aforementioned criteria, the consurf

analysis was performed for the *Hp* ND-AspRS in order to find the best position for unique restriction site introduction. Since, to date, the crystal structure of the bacterial type ND-AspRS is not available, the analysis started with generation of homology model of *Hp* ND-AspRS using the Geno3D. This automatic web server performs homology modeling for a given protein sequence by searching for homologous proteins with known crystal structures. The server then extracts geometrical restraints and builds a 3D model of the protein. The obtained 3D model was then used as a template for the consurf analysis. This online tool makes it possible to visualize functionally important region on a given protein structure by extracting the protein sequence from a given PDB file followed by sequence alignment analysis. The color coded consurf score calculated from previous step is then mapped onto the surface of the protein. Figure 1C shows results from consurf analysis of *Hp* ND-AspRS homology model. The expansion of flexible loop area revealed the less conserved alanine105 with the consurf score of 2 (The range is from 1 to 9, where 1 is the least conserved and 9 is the most conserved). This position was selected also because the introduction of *KpnI* restriction site will only require a single base mutation (C314G, *Hp* ND-AspRS numbering). The newly introduced *KpnI* site, along with pre-existing *BamHI* site in pPTC001, will facilitate the domain swapping for *Hp* ND-AspRS.

The plasmid pPC001 possessing *KpnI* was generated by means of site-directed mutagenesis. Then, the genes encoding N-terminal anticodon binding domain of *E. coli* AspRS and AsnRS were introduced into pPC001 generating pPC007 and pPC008 respectively. A brief overexpression profile analysis for Chimera-D (pPC007) and Chimera-N (pPC008) indicated the presence of soluble proteins with the molecular weight around 67 kD. Since it has been reported that the heterologous overexpression of *Hp* ND-AspRS is toxic to *E. coli* host cells, the expression of Chimera-D and Chimera-N was also conducted for 30 minutes after IPTG induction. Purified Chimera-D and Chimera-N were then subjected to the CD spectroscopic analysis in order to determine their secondary structure content. The parallel experiment was also conducted with the wild type *Hp* ND-AspRS in order to compare the CD profile between the wild type enzyme and its chimeras. The CD spectra for each protein were shown in figure 2A. In general, Chimera-D and Chimera-N provide relatively similar CD spectra compared with the wild type enzyme. The calculated secondary structure content was shown in figure 2B for each protein. These values are the average from the results generated by three separate programs, SELCON3, CDSSTR, and CONTINLL. The results also indicate only small discrepancies in the secondary structure content of the

wild type ND-AspRS, Chimera-D, and Chimera-N. Therefore, introducing the N-terminal domain from *E. coli* AspRS and AsnRS into those of *Hp* ND-AspRS gives soluble chimeric proteins with small discrepancies in secondary structure content.

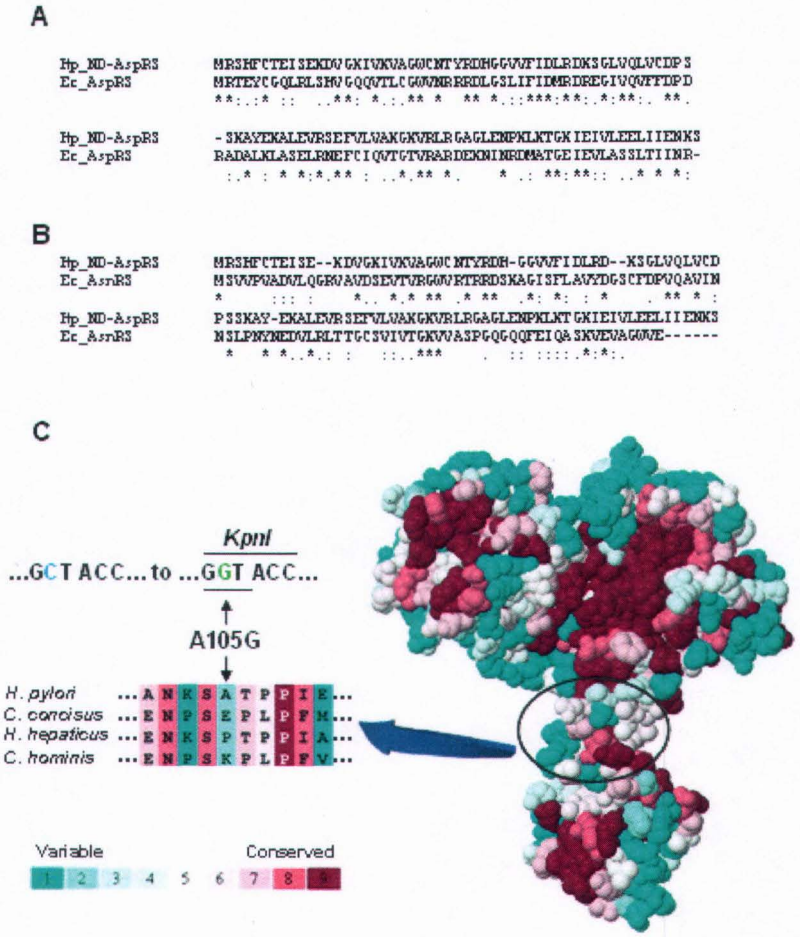

Figure 1. Rationalization for the construction of Chimera-D and Chimera-N. A) The N-terminal domain alignment for *Hp* ND-AspRS and *E. coli* AspRS. B) The N-terminal domain alignment for *Hp* ND-AspRS and *E. coli* AsnRS. C) Consurf result showing less conserved region in the hinge domain of *Hp* ND-AspRS. The alanine105 receives turquoise color code, thus represent variable position in the protein. The single base mutation was introduced in order to generate the *KpnI* restriction site. This site facilitates the introduction of N-terminal anticodon binding domain from *E. coli* AspRS and AsnRS.

A

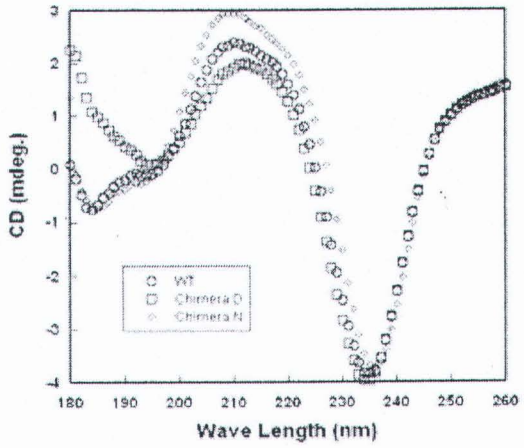

B

	Helix	Sheet	Turns	PP2	Unordered
WT	8.10	24.73	18.17	10.07	34.97
D	20.83	13.87	19.20	18.67	26.23
N	12.00	24.47	17.37	14.07	29.67

Figure 2. Circular Dichroism (CD) Analysis of Wild-type *Hp* ND-AspRS, Chimera-D, and Chimera-N. A) CD spectra overlay of Wild-type ND-AspRS, Chimera-D, and Chimera-N. B) Secondary structure content of Wild-type ND-AspRS, Chimera-D (as D in the table), and Chimera-N (as N in the table) calculated from three programs; CONTINLL, SELCON3, and CDSSTR. Values shown here are average numbers from the aforementioned programs.

The ability to form dimmer is decreased in Chimera-D, and the effect is even more pronounced in Chimera-N compare to the wild type enzyme.

Introduction of the N-terminal domain from enzymes of different organism clearly affect the ability to form homodimer of the wild-type ND-AspRS. When native-PAGE was performed under slightly denatured condition (in the presence of 0.01% SDS in running buffer), the distribution of monomer and homodimer can be observed (Figure 3.). The ability of form dimer of Chimera-D is clearly lower than the wild-type ND-AspRS. The dimerization degree in Chimera-N is the worst among three proteins analyzed. This might be the result from the incompatibility around surface area between the anticodon binding domain and the catalytic domain of the enzyme. Once can see that, introducing foreign N-terminal domain into the wild-type enzyme will also introduce the whole new set of amino acids around the contact surface of the chimeras. Therefore, it is conceivable to see such discrepancies for dimerization.

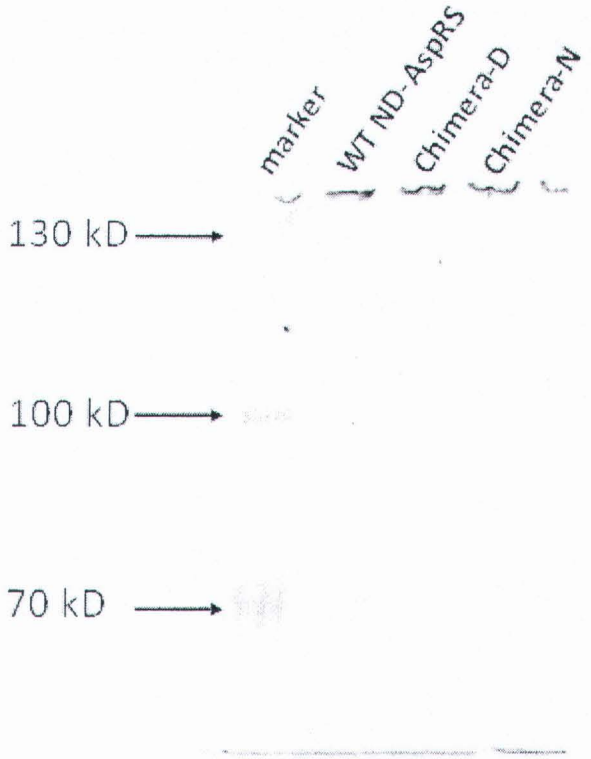

Figure 3. The Native PAGE Analysis of Wild-type *Hp* ND-AspRS, Chimera-D, and Chimera-N. The native PAGE was run in running buffer containing 0.01% SDS. Under this condition, both homodimer and monomer of the wild-type enzyme are clearly visible. The amount of dimer and monomer in each sample is significantly different. The portion of homodimer in wild-type enzyme is the highest among the three, and the lowest homodimer content is observed in Chimera-N. These results correlate well with the ability to form dimers in each protein.

สำนักงานคณะกรรมการวิจัยแห่งชาติ ห้องสมุดงานวิจัย

The tRNA^{Asp} specificity is enhanced in Chimera-D where the Chimera-N exhibit very low catalytic activity for both tRNA^{Asp} and tRNA^{Asn}.

It has been shown that the wild-type ND-AspRS prefers tRNA^{Asp} as a substrate over tRNA^{Asn}. The preference for tRNA^{Asp} over tRNA^{Asn} was evaluated using the aminoacylation assays as well as the Michaelis-Menten kinetic analysis. Then, we set forth to study tRNA specificity for our newly constructed Chimera-D and Chimera-N. As expected, both chimeras exhibit very low catalytic activity compare to the wild-type enzyme, especially in the case of Chimera-N where the aminoacylation efficiency is only slightly above the no enzyme control experiments. This observation reveals the conformational changes in Chimera-D and Chimera-N compare to the wild-type enzyme. Despite the fact that the secondary structure content in these two chimeras is approximately the same as wild-type enzyme, the conformation of these two chimeras may be different in the way that does not provide the ability to catalyze aminoacylation reaction to both tRNAs. However, the preference for tRNA^{Asp} can still be observed in the case of Chimera-D. Based on the aminoacylation assay shown in Figure 4a and b, the preference for tRNA^{Asp} in Chimera-D is clearly higher than the wild-type enzyme. Therefore, anticodon binding domain of ND-AspRS strongly contributes to its tRNA specificity. In order to quantify the contribution of this domain toward tRNA specificity, the Michaelis-Menten kinetic experiments were conducted. Unfortunately, neither of the chimeras behave well in MM kinetic experiments despite the fact that several aminoacylation conditions were explored.

สำนักงานคณะกรรมการวิจัยแห่งชาติ
ห้องสมุดงานวิจัย
วันที่ 2 ก.ค. 2555
เลขทะเบียน 245889
เลขเรียกหนังสือ

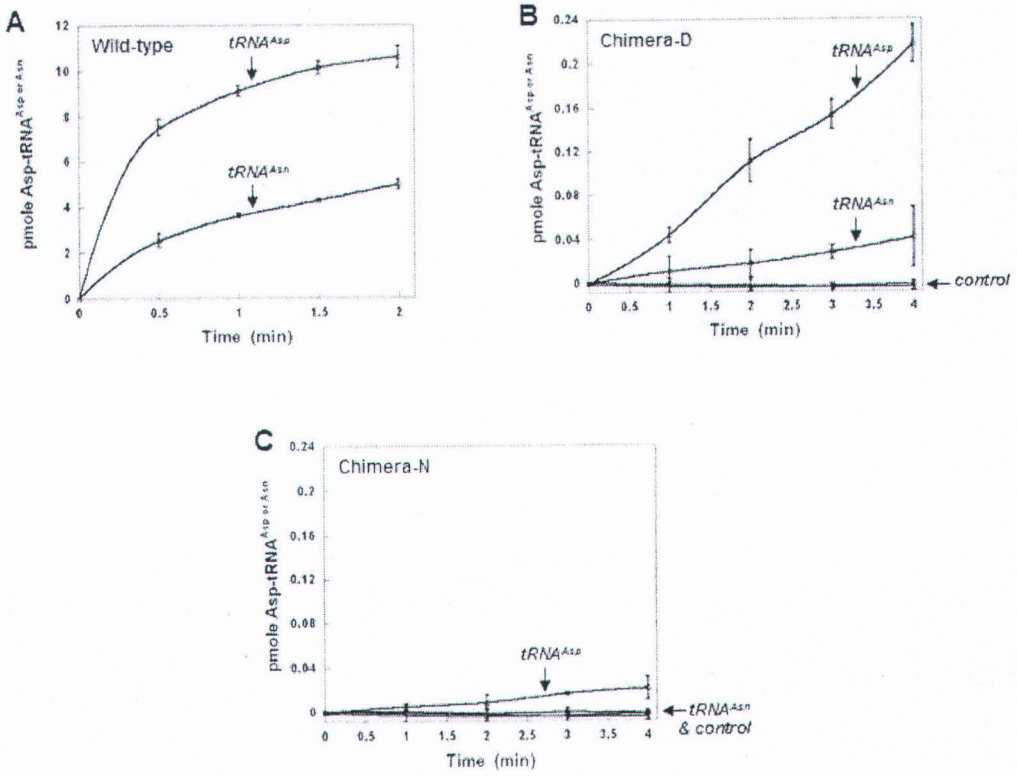

Figure 4. Catalytic Activity of Wild-type ND-AspRS, Chimera-D, and Chimera-N toward $tRNA^{Asp}$ and $tRNA^{Asn}$. The aminoacylation of $tRNA^{Asp}$ and $tRNA^{Asn}$ with wild-type ND-AspRS A), Chimera-D B), and Chimera-N C). These assays are run under identical condition (2 μM $tRNA^{Asp}$, 2 μM $tRNA^{Asn}$, and 0.2 μM enzyme)

The differences in catalytic activity and tRNA specificity of Chimera-D and Chimera-N were observed through heterologous expression of these proteins in E. coli.

Due to the fact that both chimeras are a lot less catalytically active compare to the wild-type enzyme, *in vivo* heterologous expression of these proteins in *E. coli* host cells is less toxic than those of wild-type ND-AspRS. The results in Figure 5 represent an average of experiments conducted more than 6 times in order to ensure the small difference in cell viability between those expressing Chimera-D and Chimera-N. The Chimera-N appears to be less toxic to *E. coli* host cell than Chimera-D due to its low catalytic activity compare to Chimera-D.

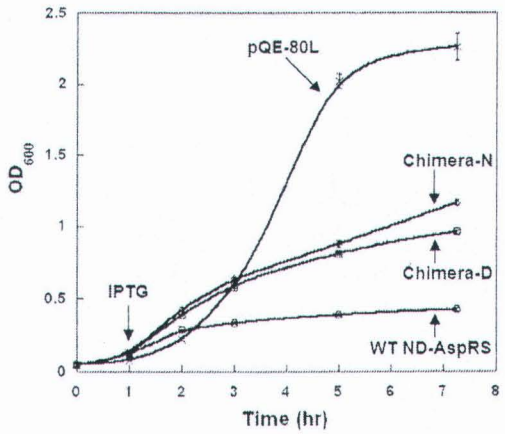

Figure 5. Heterologous Expression of Chimera-D and Chimera-N is less Toxic Than That of Wild-type ND-AspRS.